

Crystal and magnetic structures of Sm epitaxial thin films and Sm/Y superlattices

K. Dumesnil, C. Dufour, and Ph. Mangin

*Laboratoire de Physique des Matériaux (U.M.R. 7556), Université H. Poincaré, Nancy I,
Boîte Postale 239, 54506 Vandoeuvre les Nancy Cédex, France*

M. Hennion

Laboratoire Léon Brillouin, CEN de Saclay, 91191 Gif sur Yvette, France

P. J. Brown

Institut Laue-Langevin, avenue des Martyrs, Boîte Postale 156, 38042 Grenoble Cedex, France

(Received 14 December 1998)

Epitaxial Sm thin films and Sm/Y superlattices have been grown with a high single-crystal quality. The complex nine hexagonal close-packed planes stacking sequence has been successfully obtained in a 5000-Å-thick film, whose magnetic behavior presents a long-range antiferromagnetic order of the hexagonal sites below 100 K, as in the bulk element. However, from neutron scattering, the relative magnetic and nuclear contributions indicate a significant enhancement of the magnetic moment compared to the bulk value. For the superlattice, the neutron-scattering results show neither long-range structural coherence of the stacking sequence along the c direction nor a coherent magnetic ordering at low temperatures. [S0163-1829(99)15035-5]

Epitaxial thin films and superlattices of rare earths with various crystal structures, such as hexagonal-close-packed (hcp) or double-hexagonal-close-packed (dhcp), have been grown during the past decade. The epitaxial growth along the (0001) direction (c direction) has been achieved by using the method proposed by Kwo *et al.*¹ These systems exhibit very exciting magnetic properties, among them the shift of the Curie temperature,^{2,3} the coherent propagation of a helical magnetic phase through nonmagnetic or paramagnetic layers,^{4,5} and the antiferromagnetic coupling through nonmagnetic or magnetic layers.^{6,7} These effects have been attributed to epitaxial strains developed in the films by epitaxy and to the long-range polarization of the conduction electrons in the rare-earth metal.

Among the trivalent lanthanides, samarium plays a particular role between dhcp rare earths, to which corresponds the periodic stacking of four hexagonal compact planes ($ABACABAC\cdots$), and hcp rare earths which present the ($ABAB\cdots$) stacking sequence. Indeed, under normal temperature and pressure conditions, bulk samarium exhibits an intermediate crystal structure with the periodic stacking of nine hexagonal planes ($A_cB_hA_hB_cC_hB_hC_hA_hC_h\cdots$) along the c axis, giving a c parameter of 26.21 Å. This structure will be referred to as “Sm structure” in the following. The h and c subscripts recall the symmetry about the samarium atoms in each corresponding plane: the nearest-neighbor environment is approximately cubic when refereed with the letter c and hexagonal when refereed with the letter h . The magnetic structure of bulk samarium was first studied by Koehler and Moon⁸ by neutron scattering. They showed that the magnetic moments at the h sites order along the c direction at 106 K, ferromagnetically in the same basal plane with an antiferromagnetic arrangement along the c axis, resulting in a magnetic unit cell with a c axis twice as long as that of the chemical unit cell. The magnetic ordering at the c sites occurs only around 14 K, leading to a magnetic cell whose c

axis and one of the hexagonal a axes are quadrupled compared to the chemical cell (they reach 103.6 and 14.51 Å, respectively). Koehler and Moon found that the average magnetic moment per atom was close to $0.1\mu_B$, which is significantly smaller than the expected free-ion moment of $0.71\mu_B$. These authors believe that “the free ion moment is partly reduced by crystal field effects and that there is a large polarization of the conduction electrons parallel to the ionic spin. The combination of ionic plus conduction spin moments almost cancels the orbital moment which is directed in the opposite sense.” The ordering of the magnetic moment at the hexagonal sites has been confirmed recently by magnetic x-ray resonant scattering.⁹ This technique is also very promising to separate the orbital and spin contributions, which are in competition in the magnetic moment.

In its trivalent electronic configuration, the structure of samarium metal is sensitive to pressure and temperature, as shown in the phase diagram proposed by Coles,¹⁰ and it can therefore adopt one of the other common hexagonal plane stacking: hcp, dhcp, or fcc. Recent experiments performed by Adachi *et al.*¹¹ on hcp samarium quenched from the melt have shown that hcp samarium is a ferromagnet with a Curie temperature of 165 K and, as in the Sm structure, the magnetic moment has been estimated to $0.1\mu_B$. The lattice parameters for this hcp stacking are $a=3.65$ Å and $c=5.80$ Å, which corresponds to a c axis d spacing 0.42% smaller than in the Sm structure.

Moreover, because of the weak energy difference between the two electronic configurations $(4f)^5(5d5s)^3$ and $(4f)^6(5d5s)^2$, the samarium is subject to a change of valence between Sm^{3+} and Sm^{2+} . The valence state is very sensitive to the surrounding of the atoms, either in alloying or at the surface. It has been extensively demonstrated that the surface of samarium was divalent¹² and that the hexagonal 5×5 surface reconstruction observed at low temperature was related to the valence of the surface atoms.¹³ In the same

way, it has been observed by Mason *et al.*¹⁴ that samarium could be divalent in small grains where the surface effects are dominating.

In this context, the study of epitaxied samarium-based systems, such as thin films or superlattices, arises to be of particular interest. Various points would need to be investigated, and first the crystal structure of samarium in layers where epitaxial strains and surface (interface) effects can be important: is it possible to grow a long-range coherent samarium structure, and to tailor the crystal structure via epitaxial strains or in changing elaboration parameters, such as the substrate temperature during deposition or the deposition rate? What will be the hexagonal planes stacking sequence and its coherence in superlattices constituted of samarium metal and of another rare earth (RE) with a different structure (Sm/hcp-RE or Sm/dhcp-RE superlattices), especially in samples where the thickness of the samarium layers is only some unit cells? Concerning the magnetic properties, is it possible to get a long-range-ordered magnetic structure, in thin films as well as in superlattices?

In this paper, we present structural and magnetic results showing some aspects of the samarium behavior in epitaxial thin films and superlattices.

EXPERIMENTAL TECHNIQUES

The samples were prepared by molecular beam epitaxy in an ultrahigh-vacuum chamber whose base pressure typically reaches 4×10^{-11} Torr. Following the usual process to grow (0001) rare-earth epitaxied systems, a (11 $\bar{2}$ 0) single-crystal sapphire is used as a substrate and first covered with a thick niobium buffer deposited at 820 °C. Samarium and yttrium are then evaporated from an effusion cell and an electron gun, respectively. During this deposition process, the substrate is kept at 280 °C. This relatively low temperature has been chosen to avoid reevaporation of samarium and interdiffusion in the case of superlattices. *In situ* reflection high-energy electron diffraction (RHEED) experiments evidence the single-crystal quality of the deposited layers and permit us to identify the *c* axis as the growth direction. Moreover, the in-plane surface parameter measured by RHEED appears to be significantly larger than the bulk samarium parameter.¹⁵ This is consistent with previous observations, and has been related to the divalent character of the Sm surface.¹² The true compositions of the superlattice samples were determined from a combination of x-ray diffraction (for the superlattice period) and fluorescence x-ray analysis (for the atomic fractions). The samples discussed in this paper are a 5000-Å-thick samarium film and a [145 Å Sm/120 Å Y]₁₀ superlattice.

The structural and magnetic properties have been investigated both by high-angle x-ray-diffraction and neutron-scattering experiments. These latter have been performed on the 4F.1 triple axis instrument in the Laboratoire Léon Brillouin (CEN, Saclay). The neutron wavelength was 4.245 Å, which leads to an instrumental resolution of 0.0102 Å⁻¹ for the scattering vector along the *c** direction. Higher-order contamination was suppressed using a beryllium filter. Samples were cooled using a closed-cycle refrigerator and measurements were taken over the temperature range 50–300 K.

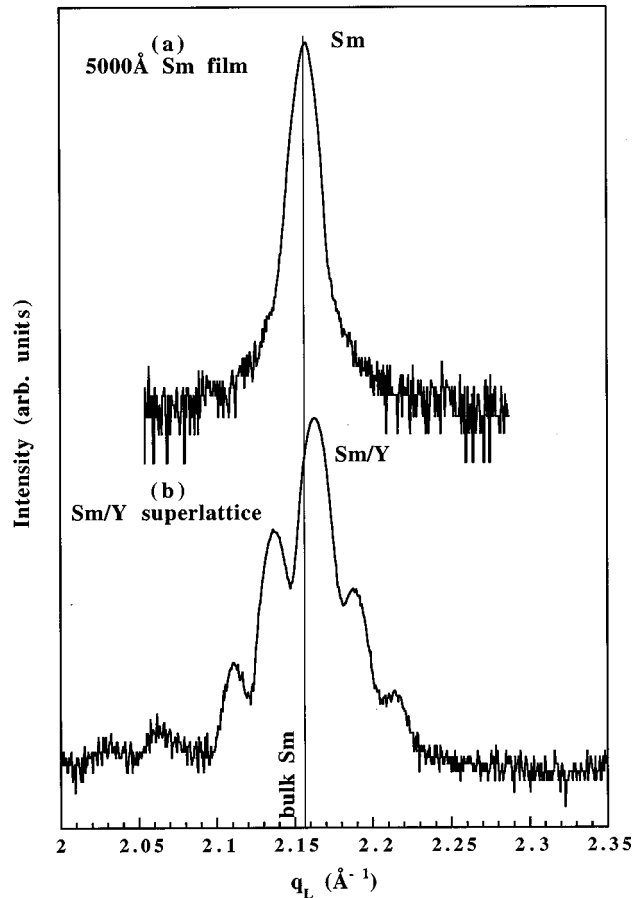


FIG. 1. Room-temperature x-ray-diffraction patterns with the wave-vector transfer along the [00 l] direction for (a) a 5000-Å-thick samarium film, (b) a Sm (145 Å)/Y (120 Å) superlattice.

CRYSTAL STRUCTURES

Figure 1 presents typical x-ray-diffraction patterns collected at room temperature with the wave-vector transfer along the [00 l] direction for the 5000 Å-thick samarium film [Fig. 1(a)] and the Sm/Y superlattice [Fig. 1(b)]. The scan 1(a) exhibits a sharp peak at $Q = 2.152 \text{ \AA}^{-1}$, which corresponds to the reflection of the hexagonal-close-packed planes (separated by 2.912 Å) perpendicular to the *c* axis. However, it is impossible in this geometry to determine the positions of ions within the close-packed planes, that is, to distinguish between the different stacking sequences: Sm structure, hcp, or dhcp. The observed peak would be referred to as (009)_{Sm} for the Sm structure, (002)_{hcp} for the hcp structure, or (004)_{dhcp} for the dhcp one. We can just point out that the distance between close-packed planes is slightly closer to the value expected from the Sm structure ($26.21/9 = 2.912 \text{ \AA}$) than from the hcp stacking ($5.8/2 = 2.9 \text{ \AA}$). The coherence length of the stacking of close-packed planes in the growth direction, deduced from the full width at half maximum of the peak, was found to be about 700 Å, which is similar to the coherence length we have usually measured in thin epitaxied films of other rare earth. A transverse scan through the Bragg peak yields a mosaic spread of approximately 0.13°, which reveals a good crystal quality of the samarium film.

For the Sm/Y superlattice, the scan shown in 1(b) exhibits an average main Bragg peak surrounded by satellites, whose position gives the bilayer repeat distance (265 Å). Their presence attests for a long-range structural coherence i.e., a

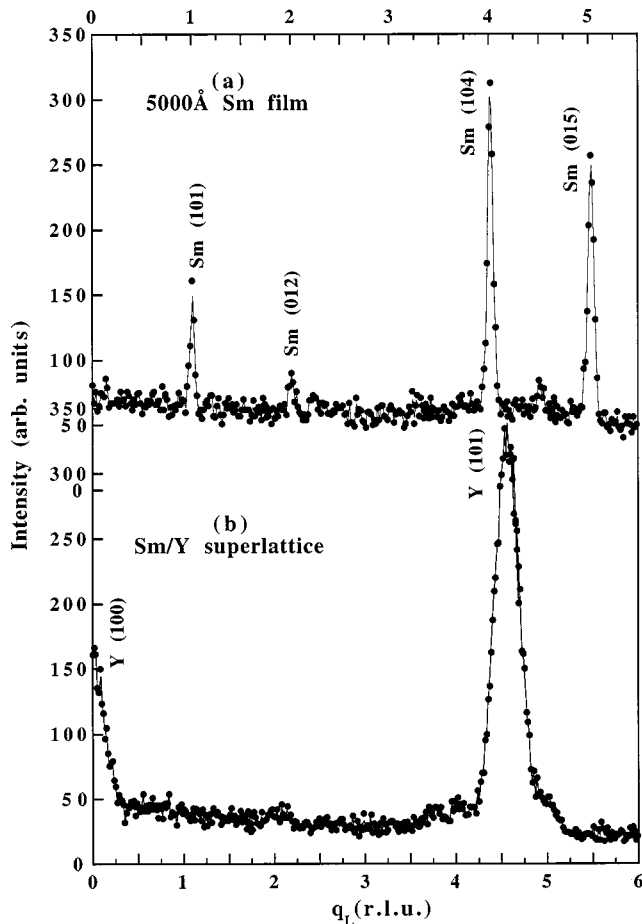


FIG. 2. Room-temperature neutron-scattering spectra with the wave-vector transfer along the $[10l]$ direction for (a) a 5000-Å-thick samarium film, (b) a Sm (145 Å)/Y (120 Å) superlattice.

periodic alternation of close-packed yttrium and samarium planes, independent of the sequence. The main Bragg peak, which is an average of both the samarium and yttrium contribution, is significantly shifted from the bulk $(009)_{\text{Sm}}$ Bragg peak, as it could be expected. The coherence length deduced from the width of the main peak (0.0127 \AA^{-1}) is about 500 Å, and the mosaic spread deduced from a transverse scan through the Bragg peak is 0.27° .

The actual crystal structure can be deduced from scans with the wave-vector transfer along the $[10l]$ direction, providing information on the stacking sequence of the close-packed planes along the c axis: In reciprocal-lattice units referred to the Sm structure, the hcp structure would give rise to a $(101)_{\text{hcp}}$ peak at $(1\ 0\ 4.5)_{\text{Sm}}$, the dhcp structure would give $(101)_{\text{dhcp}}$ and $(102)_{\text{dhcp}}$ peaks, respectively, at $(1\ 0\ 2.25)_{\text{Sm}}$ and $(1\ 0\ 4.5)_{\text{Sm}}$, and the Sm structure would be characterized by $(101)_{\text{Sm}}$, $(012)_{\text{Sm}}$, $(104)_{\text{Sm}}$, and $(015)_{\text{Sm}}$ peaks. These four peaks arising from the Sm crystal structure can be present all together along the $[10l]$ direction, if there is a coexistence of domains rotated by 120° .

The neutron-diffraction pattern measured at room temperature along the $[10l]$ direction for the 5000-Å-thick Sm film is presented in Fig. 2(a) (in reciprocal-lattice units with respect to the Sm structure). All the peaks unambiguously reveal that the crystal structure is similar to that of bulk samarium with a nine close-packed planes stacking sequence. The absence of diffraction peaks between $(104)_{\text{Sm}}$

and $(015)_{\text{Sm}}$ excludes the presence of some hcp or dhcp structure. The fact that these peaks are narrow shows that the stacking sequence is coherent over 480 Å (18 unit cells), which is slightly smaller than the coherence length of the basal planes measured in the $[00l]$ direction (700 Å). However, such a perfect Sm structure was not systematically obtained. Several Bragg peaks typical of a mixture of dhcp and Sm crystal structures have been observed in some epitaxial films, under different preparation conditions, such as the substrate temperature during the deposition or the evaporation rate. The relevant parameters deciding between one crystal structure or the other still have to be determined via a more systematic study.

Figure 2(b) presents the scan along $[10l]$ measured at room temperature for the Sm/Y superlattice. Mainly broad peaks are observed at the $(100)_{\text{hcp}}$ and $(101)_{\text{hcp}}$ positions, with two faint bumps at the $(104)_{\text{Sm}}$ and $(015)_{\text{Sm}}$ positions. Complementary x-ray-scattering experiments have also revealed a broad peak at the $(0\ 1\ 14)_{\text{Sm}}$ position. The width of the peaks indicates that the associated structural coherence lengths are around 100 Å, comparable to the thickness of the individual layers. In contrast to the results obtained along the $[00l]$ direction (either by x-ray or neutron scattering), there are no sharp peaks surrounded by satellites, which means that the hcp- and Sm-stacking sequences along the c direction are not periodic and their coherence is confined to individual blocks. It is likely that the $(100)_{\text{hcp}}$ and $(101)_{\text{hcp}}$ peaks are mainly due to the hcp Y, and the other contributions are mainly due to the nine-plane stacking of Sm. We can therefore conclude that the Y layers present a hcp stacking and the Sm layers present a nine-plane stacking, as in the bulk elements. However, we assume that the samarium layers contain stacking faults from the Sm structure, which gives rise to such faint bumps at the $(104)_{\text{Sm}}$ and $(015)_{\text{Sm}}$ positions.

It should be noted that this structure is similar to what occurs in the Nd/Y superlattices,¹⁶ where the hcp and dhcp structures are obviously kept in the Y and Nd layers, respectively, with coherence lengths limited to the layer thicknesses.

MAGNETIC STRUCTURES

Figure 3 presents the neutron-scattering pattern measured at 50 K for the samarium film along the $[10l]$ direction, with the room-temperature spectrum for comparison. Several new peaks (indicated by arrows) are present at low temperature, the more intense ones being located at the positions $(1\ 0\ 7/2)_{\text{Sm}}$ and $(1\ 0\ 11/2)_{\text{Sm}}$, which corresponds to a doubling of the unit cell along the c direction. They are typical of the antiferromagnetic ordering of the h sites, described by Koehler and Moon.⁸ The temperature dependence of the magnetic intensity (see inset in Fig. 3) leads to T_N near 100 K, which is close to the samarium bulk Néel temperature (106 K).

The integrated intensities of the magnetic peaks have been scaled with respect to those of the nuclear peaks. The results indicate that the magnetic scattering from the samarium film is between five and ten times larger than that determined for a bulk sample by Koehler and Moon.⁸ This cannot simply be interpreted as showing that the magnetic moment in the film is greater by a factor 3 than that in the bulk, since the mag-

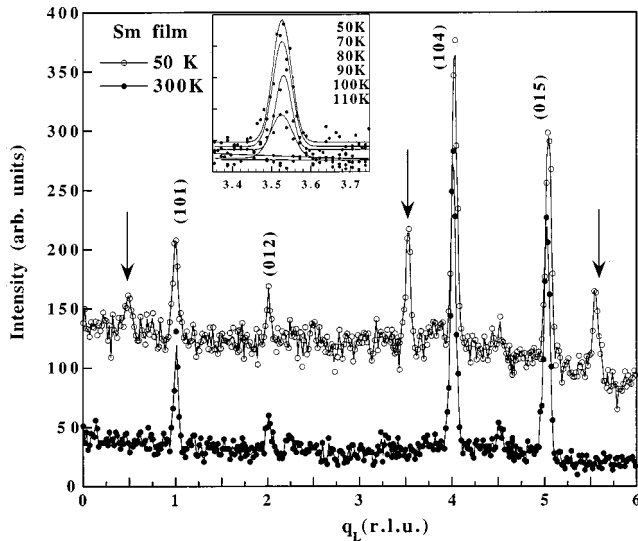


FIG. 3. Neutron-scattering spectra collected at 300 and 50 K with the wave-vector transfer along the $[10l]$ direction for the 5000-Å-thick samarium film. The arrows indicate the magnetic satellites. The inset presents the thermal evolution of the $(1\ 0\ 7/2)$ magnetic peak.

netic moment of samarium arises from a delicate balance between oppositely directed spin and orbital moments. The intensities of the three magnetic peaks which were observed have been fitted to the Koehler and Moon structure using the dipole approximation to the samarium form factor:

$$f_{\text{Sm}}(q) = \langle j_0(q) \rangle (L + 2S) + \langle hj_2(q) \rangle L,$$

where $\langle j_0(q) \rangle$ and $\langle j_2(q) \rangle$ are the form-factor integrals calculated for Sm^{3+} by Freeman and Desclaux.¹⁷ If it is assumed that L has its maximum value $L=5$, we obtain $S = 1.9 \pm 0.1$ and a resultant magnetic moment of $1.2 \pm 0.2 \mu_B$.

For the superlattice, the intensity of the broad Bragg peaks was practically kept unchanged upon decreasing temperature, and we did not observe the emergence of any extra

peaks typical of a magnetic ordering along the $[10l]$ direction. The only temperature dependence is a slight shift in the Bragg peaks positions, due to the thermal contraction of the lattice parameters. Nevertheless, because of the extremely large samarium neutron absorption cross section, we assume that the absence of magnetic satellites in this superlattice does not have to be immediately interpreted as a nonmagnetic ordering in the individual samarium layers. Namely, if the magnetic order sets in without any coherence between successive layers, the magnetic contribution is expected to present a large full width at half maximum; it is thus certainly impossible to extract it from the high background.

In this first paper devoted to samarium epitaxial layers and to Sm/Y superlattices, we have shown that it is possible to grow (0001) single-crystal systems with a high-quality complex samarium crystal structure. However, some samples gather both the samarium and the dhcp structures, and the precise relevant parameters governing the crystal structure are still under investigation. As in the bulk element, we observed that the Sm samples exhibit an antiferromagnetic ordering at the h sites near 100 K. Nevertheless, the magnetic moment appears to be larger than the expected value from the bulk samarium investigation ($1.2 \mu_B \pm 0.2$ instead of $0.1 \mu_B$).

Sm/Y superlattices have been also grown with a very good crystal quality; they present a stacking of hexagonal-close-packed samarium and yttrium planes, in which the hexagonal planes are perpendicular to the growth direction. However, these samples do not exhibit long-distance coherence of the stacking of the atomic planes. Yttrium and samarium exhibit their specific stacking sequence in each layer without any coherence between layers.

We are currently going on with the elaboration work, especially in trying to control the stacking of the atomic planes. On the other hand, neutron and resonant magnetic x-ray-scattering experiments are about to be performed, in order to separate the orbital and spin contributions, to determine the ordering of the c sites at low temperature, and to investigate the effects related to the conduction-electron polarization in these samarium systems.

¹J. Kwo, M. Hong, and S. Nakahara, Appl. Phys. Lett. **49**, 319 (1986).

²K. Dumesnil, C. Dufour, Ph. Mangin, G. Marchal, and M. Hennion, Europhys. Lett. **31**, 43 (1995).

³F. Tsui and C. P. Flynn, Phys. Rev. Lett. **71**, 1462 (1993).

⁴R. W. Erwin, J. J. Rhyne, M. B. Salamon, J. Borchers, S. Sinha, R. Du, J. E. Cunningham, and C. P. Flynn, Phys. Rev. B **35**, 6808 (1987).

⁵K. Dumesnil, C. Dufour, Ph. Mangin, G. Marchal, and M. Hennion, Phys. Rev. B **54**, 6407 (1996).

⁶R. S. Beach, J. A. Borchers, A. Matheny, R. W. Erwin, M. B. Salamon, B. Everitt, K. Pettit, J. J. Rhyne, and C. P. Flynn, Phys. Rev. Lett. **70**, 3502 (1993).

⁷K. Dumesnil, C. Dufour, M. Vergnat, G. Marchal, Ph. Mangin, M. Hennion, W. T. Lee, H. Kaiser, and J. J. Rhyne, Phys. Rev. B **49**, 12 270 (1994).

⁸W. C. Koehler and R. M. Moon, Phys. Rev. Lett. **21**, 1469 (1972).

⁹S. L. Lee, E. M. Forgan, S. J. Shaikh, C. C. Tang, W. G. Stirling, S. Langridge, A. J. Rollason, M. M. Costa, M. J. Cooper, E. Zukowski, J. B. Forsyth, and D. Fort, J. Magn. Magn. Mater. **127**, 145 (1993).

¹⁰B. R. Coles, J. Less-Common Met. **77**, 153 (1981).

¹¹H. Adachi, K. Kimura, and H. Ino, Mater. Sci. Eng., A **181**, 864 (1994).

¹²J. W. Allen, L. I. Johansson, R. S. Bauer, I. Lindau, and S. B. M. Hagström, Phys. Rev. Lett. **41**, 1499 (1978).

¹³A. Stenborg, J. N. Andersen, O. Björneholm, A. Nilsson, and N. Martensson, Phys. Rev. Lett. **63**, 187 (1989).

¹⁴M. G. Mason, S. T. Lee, G. Apai, R. F. Davis, D. A. Shirley, A. Franciosi, and J. H. Weaver, Phys. Rev. Lett. **47**, 730 (1981).

¹⁵K. Dumesnil, C. Dufour, and Ph. Mangin (unpublished).

¹⁶B. A. Everitt, M. B. Salamon, J. A. Borchers, R. W. Erwin, J. J. Rhyne, B. J. Park, K. V. O'Donovan, D. F. McMorro, and C. P. Flynn, Phys. Rev. B **56**, 5452 (1997).

¹⁷A. J. Freeman and J. P. Declaux, J. Magn. Magn. Mater. **12**, 11 (1978).